OXYGEN AND HYDROGEN DIFFUSION IN ZIRCONIA

B. SZPUNAR†, M.I. BASKES‡ and P.T. JOCHYM#

Royal Military College of Canada, Department of Chemistry and Chemical Engineering,
P.O. Box 17000 St. Forces, Kingston, Ontario, K7K 7B4, CANADA
† Currently: Fuel & Fuel Channel Safety Branch, AECL, Chalk River Laboratories
Chalk River, Ontario, Canada K0J 1J0
‡ Los Alamos National Laboratory MS G755, Los Alamos, NM 87545, USA
# Institute of Nuclear Physics, ul. Radzikowskiego 152, 31-342 Cracow, POLAND

ABSTRACT

The ability of oxygen and hydrogen atoms to diffuse through the oxidized Zircaloy sheath on CANDU fuel elements under accident conditions is investigated with a molecular-dynamics approach, employing the Modified Embedded Atom Method (MEAM). Improved MEAM potentials (that include angular forces and are therefore suitable to study nonmetallic systems like oxides) for the ternary system Zr-O-H were developed in this work.

INTRODUCTION

This work is an extension of a previous study on model development and simulation of small-scale experiments - performed to improve our understanding of the fundamental processes affecting fission-product release from CANDU fuel elements under accident conditions [1]. The previous simulations indicated [1] that to account for the experimentally observed enhanced release kinetics of fission products, after the completion of sheath oxidation, greater exchange of steam in the fuel-sheath gap has to be assumed. These simulations therefore adopted a cracked-oxide model, but the effect of diffusion in zirconia sheath (without cracks) has to be investigated. The diffusion of hydrogen and oxygen atoms through oxidized cladding can affect the oxygen potential, and hence the release behavior of fission products from the fuel matrix of fuel elements under accident conditions [1]. The zirconium-alloy cladding forms an oxide by reaction with steam. The oxide layer becomes porous on a microscopic scale and cracked on a macroscopic scale and that offers much less resistance for oxygen transport [2]. To account for this enhanced oxygen transport, and the subsequent increased cesium release that results from the oxidized urania, a simple cracked-oxide model was proposed in our earlier simulations [1].

If the oxide layer were completely intact and protective, oxygen transport through the layer would be more restricted and could only occur by solid-state diffusion. In the present work, the possibility that the unbreached oxidized cladding can act as a physical barrier to hydrogen and oxygen diffusion was further investigated by atomistic simulation. The initial studies of oxygen and hydrogen diffusion in zirconia were presented in our earlier molecular-dynamics simulations [3] with the use of a rough semiempirical potential, because of the limited availability of the necessary experimental data used in the fitting parameters of the model. To account for the lack of experimental data in the present studies, the elastic constants of ZrH_2 and ZrO_2 were calculated using the simple deformational method [4] based on the results of VASP (Vienna Ab-initio Simulation Package) code *ab initio* calculations.

Detailed studies of hydrogen and oxygen diffusion through zirconia cladding were carried out using a molecular-dynamics (MD) approach, with the interactions between atoms represented by Modified Embedded Atom Method (MEAM) potentials [5]. The MEAM is an empirical extension of the embedded atom method (EAM) that includes angular forces and is therefore suitable for studies of nonmetallic systems like oxides. The parameters of the MEAM potentials for the Zr-H-O system are fitted to predict the elastic properties of zirconia and zirconium hydride in agreement with *ab-initio* calculations.

This work also finds application in the investigation of perovskite-based, high-temperature, protonic conductors, which are possible new materials for fuel cells [6]. It is of interest to study hydrogen diffusion in zirconium dioxide since it is related to these protonic conductors.

MODIFIED EMBEDDED ATOM POTENTIALS FOR THE Zr-O-H SYSTEM

MEAM potentials for the ternary system Zr-O-H are developed here. The parameters for the individual elements have previously been developed by Baskes and Johnson [7] for Zr, and Baskes [5] for O and H. The original parameters for Zr are modified slightly to use a face centered cubic (fcc) reference structure and to use the following form for the background electron density:

$$\bar{\rho} = \sqrt{\sum_{l=0}^{3} t^{(l)} \rho^{(l)^2}} \qquad (1)$$

where the $t^{(l)}$ are parameters and the $\rho^{(l)}$ are partial electron densities [5]. The parameters for O and H are taken directly from Ref. [5] but the atomic density scaling ρ_0 is modified. All of the parameters for the elements are given in Table 1. The reference states for the ZrO and ZrH systems are chosen to be B3 (zinc blende). For the OH system, the dimer is taken to be the reference state. The parameters that define the universal binding energy relationship (UBER) [8] are given in Table 2. Angular screening is implemented as in Huang et al. [9] with parameters $C_{min} = 1.2$ for Zr-Zr-Zr screening and $C_{min} = 2.0$ for all other combinations of atoms. The cut off radius for the potential was chosen to be 4.5 Å.

The parameters in Tables 1 and 2 are used to calculate the lattice constants and the cohesive energies of cubic ZrO_2 and ZrH_2 which are shown in Table 3. There is good agreement between the predicted and experimental values. The unit cell for ZrO_2 is depicted in Figure 1. Pure zirconia has a monoclinic structure at low temperatures, but above 1400°C, or when stabilized by adding impurities of Ca or Y, the cubic fluorite structure becomes stable [10]. The current simulations with the MEAM potential predict the cubic phase of zirconia to be stable (for all temperatures) but this is not important because only results at a high temperature (1700 K) are discussed here. This analysis also predicts that ZrH_2 does not remain tetragonal but rather transforms to a cubic structure (i.e., with the same volume as the tetragonal phase) with lattice constants slightly smaller than that of zirconia (Table 3).

The experimental binding energies have been calculated as a sum of the experimental heat of formation (equal to 11.4 eV/cell [12] and 1.7 eV/cell [13], respectively for zirconia and zirconium hydride) plus the binding energies of zirconium (6.36 eV [14]) and diatomic molecules (O_2: 5.14 eV and H_2: 4.50 eV respectively) [15]. These parameters underestimate the energy of formation of an H_2O molecule by 50% (4.82 eV versus 9.634 eV), and predict that the bond angle is 180° (versus experimental 100.115°[15]) with a slightly longer bond length (1.055 Å versus 0.974 Å [15]). Previous *ab initio* calculations for transition metal hydrides [16] indicate that electrons associated with hydrogen atoms form a hydrogen-metal bonding state with negligible charge redistribution (which is different from that of covalent bonding in H_2O). Consequently, the parameters (in particular ρ_0) have to be adjusted to model the H_2O molecule but this is beyond the current simulations. Also calculated are the energies of Zr, O, H single-atom vacancies and divacancies of the nearest neighbor atoms: Zr-A (where A means an O or H type of atom). The energies of single-atom vacancies, as presented in Table 3 (24.36 and 11.33 eV), are smaller than those obtained in previous simulations for the energies of defects in ZrO_2 (with an ionic-type potential) [17], i.e., 86.062 eV for a zirconium vacancy and 14.771 eV for an oxygen vacancy. The corresponding trends, however, are similar. The energy of the Schottky defect (32.49 eV) is larger than the one obtained before (1.969 eV) [17] and is slightly smaller than the sum of the energies of defects for single atoms (35.69 eV).

Elastic Properties

In fitting MEAM parameters, the elastic constants calculated by the *ab initio* method are used. The elastic constants of ZrH_2 and ZrO_2 have been calculated using the simple deformational method described in the earlier work [4], which is based on results of *ab initio* calculations of the stress tensor of the undeformed and deformed lattices. The Density Functional Theory *ab initio* calculation was carried out using the plane-wave basis set approach implemented in the VASP code. The reciprocal space sampling convergence was tested with various sampling grids, from 3x3x3 up to 12x12x12 wave vectors in the irreducible Brillouin zone. A sufficient convergence was obtained for energies and forces (10^{-6} eV and 10^{-5} eV/Å, respectively).

Table 4 shows the calculated results for the bulk, shear, Young's modulus and elastic constants at 0 K for ZrO_2 and ZrH_2. For the *ab initio* calculations, bulk modulus was also calculated using an alternative formula (values inside the parenthesis):

$$B = -V dP / dV \qquad (2)$$

where V is the volume at the pressure P.

The elastic constants calculated using VASP and MEAM are in agreement with each other. They are also in qualitative agreement with the experimental data presented in Table 4. In particular, the c_{11} constant is between 4 and 5 times larger than the c_{12} constant and the c_{44} constant is about 50% smaller than the c_{12} constant. The low-temperature phase of zirconia is monoclinic, and it is difficult to measure elastic constants at the high temperatures where the cubic phase is stable. Therefore, we included the results for the elastic constants with derived bulk and shear moduli (values extrapolated from cubic Y_2O_3–doped zirconia data to pure zirconia) [18], as well as the Young's and shear moduli for monoclinic zirconia [19], with the averages over different directions of elastic constants for the monoclinic phase [21]. The Potential Induced Breathing (PIB) model, based on the charge density calculated values by the linearized augmented plane wave method [22], predicts a bulk modulus equal to 288 GPa and a shear modulus of 189 GPa for cubic zirconia, which is larger than calculated here by both the *ab-initio* and MEAM approximation methods (Table 4). The c_{11} (560 GPa) elastic constant obtained by the PIB [23] method agrees with those calculated here (489 GPa and 482 GPa), but the c_{44} (180 GPa) and c_{12} (153 GPa) elastic constants are much larger than the corresponding values in Table 4. In agreement with the experimental measurements and *ab initio* calculations (Table 4), the MEAM approximation (in contrast to a pure pair potential prediction) predicts c_{12} and c_{44} to be different due to an embedding energy term and angular terms in the potential.

MOLECULAR DYNAMICS SIMULATION

The MD simulations were performed for a slab of ZrO_2 with 288 atoms and periodic boundary conditions in the z and y directions. The (110) surface (indicated in Figure 1) has been chosen since it is a more stoichiometric surface than, for example, the (100) surface. The initial relaxations (until 1700 K temperature was reached) were performed for an equivalent bulk structure. Then the surface was created by increasing the periodic length in the x direction. This procedure creates a rough surface due to the relatively large amplitude of vibrations of atoms at 1700 K. The current simulation was performed in order to investigate whether the oxidized cladding can act as a physical barrier to either oxygen or hydrogen diffusion at the temperature of the annealing experiment (i.e., 1700 K). The oxygen or hydrogen atoms were initially positioned outside the slab at a distance shorter than the radius of the cut-off potential. The current simulation (time step equal to 0.0005 ps and 6300 ps simulations time) indicates that while oxygen diffuses into the bulk through the (110) surface, it does not diffuse through the layer but stays close to the surface. The diffusion of other oxygen atoms was investigated and it was found that atoms in the bulk slab do not diffuse, but oxygen atoms on the surface diffuse along the surface. In Figure 2 a-b the x (a) and y (b) coordinates (as a function of time) of one of the oxygen atoms on the surface are shown. The x coordinate varies only due to the thermal vibration and the y coordinate changes as the atom migrates along the surface. The temperature shows oscillations as a function of time but the mean value stays the same and it is equal to 1700 K.

Hydrogen diffusion on the surface was investigated next by replacing the oxygen atom residing in front of the (110) surface with a hydrogen atom. The time step was reduced to 0.00001 ps since the mass of the hydrogen atom is small. It was observed that (at simulated 1700 K temperature) hydrogen is occasionally kicked out from the surface by thermal excitations and travels through the vacuum to the next available surface due to the periodic boundary condition. Alternatively, it can diffuse along the surface. Eventually, hydrogen becomes trapped (for up to 20 ps) by oxygen atoms at the surface.

Simulations of the diffusion of oxygen and hydrogen atoms in bulk zirconia were then performed. Clusters consisting of an ideal structure of zirconia with 324 atoms were created. Oxygen diffusion was studied in a cluster without any defects, a cluster with 22 oxygen vacancies (10%), and a cluster with 1 zirconium atom vacancy and 22 oxygen vacancies. The current analysis indicates that oxygen does not diffuse in zirconia unless zirconium atom vacancies are present. Even with 10% oxygen vacancies, no diffusion was observed during a 10 ns simulation with a time step of 1×10^{-3} ps.

The situation is quite different when a hydrogen atom is embedded in ZrO_2 bulk at 1700 K. During the simulation time (2600 ps) hydrogen diffuses easily through the lattice. The average temperature is 1700 K with some oscillations around the required temperature during simulation time.

The calculated diffusion constant for oxygen atoms on the surface (with a time step equal to 0.0005 ps and total simulation time of 6 ns) is $1.8\times10^{-11}m^2/s$. There are not enough statistics to calculate the diffusion constant of the oxygen atom in the cluster with one Zr vacancy (time step equal to 0.001 ps and total simulation time equal to 14 ns). However, for the cluster with 6 Zr vacancies (maximum time 6 ps) the average (over 3 atoms with the highest diffusion constant) is $13.5\times10^{-13}m^2/s$. The calculated diffusion coefficient in the bulk (with vacancies) is two orders of magnitude smaller than on the surface. These values are much less than the experimentally measured diffusion constant for polycrystalline zirconia ($D = 4\times10^{-9}\ m^2/s$ at 1700 K) [24].

The current analysis suggests that for pure zirconia, experimentally observed oxygen diffusion must take place via defects (e.g. cracks, porosities) where gas diffusion may play the role. Oxygen diffusion has been studied in highly dense nanocrystalline ZrO_2 [25]. It has been found that the diffusion of oxygen in interfaces is three to four orders of magnitude faster than volume diffusion within the entire temperature range studied (720-1220 K).

Extrapolated to 1700 K, the diffusion constants are $4.15\times10^{-14}m^2/s$ and $5.57\times10^{-11}m^2/s$ for the bulk and interface diffusion of oxygen, respectively. The effect of the phase change to a cubic structure is neglected here, which can be justified because the density does not change much at the phase transition [10]. These values are in quantitative agreement with current calculations even though the diffusion constant was measured for the monoclinic phase. It has been noticed that diffusivity of oxygen in undoped monoclinic ZrO_2 is in comparison to the melting temperature, much higher than in other transition metal oxides (e.g., TiO_2, which is chemically very similar to zirconia, has extrapolated bulk diffusion of oxygen at 1700 K equal to $9.75\times10^{-15}m^2/s$). This has been attributed to the instability of the monoclinic phase of zirconia, which at higher temperature transforms to the more dense fluorite structure [25].

The molecular dynamics simulations presented here are unable to reproduce this effect by predicting a stable fluorite structure for all temperatures. The measured activation energy (2.3 eV) for the bulk oxygen diffusion in undoped monoclinic ZrO_2 is nearly twice as high as in Y_2O_3 or CaO stabilized zirconia (0.9-1.3 eV). The enhanced diffusion (of the oxygen atoms) in doped zirconia is controlled by the migration of structural oxygen vacancies [26]. Further *ab initio* calculations are necessary in order to better understand the diffusion behaviour of oxygen in zirconia. In particular, the effect of divalent (e.g. Mg^{2+}) and trivalent (Y^{3+}) ions (which are usually incorporated into the zirconia structure to stabilize the cubic phase) should be studied. They create a number of oxygen vacancies and an electronic charge disturbance, which may enhance the diffusion of oxygen.

The possibility of protonic conduction in oxides was suggested some time ago [27] and the existence of protons in ZrO_2 in a hydrogen-containing atmosphere was studied. It was expected, however, that protonic conductivity of zirconia for temperatures below 1300 K would be quite low compared to those of low-temperature conductors [27].

A cluster of 324 atoms has been created and relaxed at 1700 K to study hydrogen diffusion at constant pressure in defect-free zirconia. The total simulation time was 5000 ps with a time step equal to 0.0001 ps. A hydrogen atom with a zero initial velocity was positioned interstitially. The analysis indicates that once hydrogen is in the zirconia lattice, it can diffuse easily by random jumps and the calculated diffusion constant is $1.2\times10^{-9}m^2/s$ at 1700 K. This value is one order of magnitude lower than the measured diffusion constant of hydrogen in metallic zirconium extrapolated to 1700 K ($2.97\times10^{-8}m^2/s$ [28] and $2.99\times10^{-8}m^2/s$ [29]), but it is much higher than the measured diffusion constants for polycrystalline dense oxides extrapolated to 1700 K (again the monoclinic – cubic phase transition is neglected): ZrO_2 film on Zr ($9.328\times10^{-16}m^2/s$ [30] and ZrO_2 film on Zr-2.5 Nb ($6.72\times10^{-15}m^2/s$ [30]). The reason for the difference between the measured diffusion constants in ZrO_2 films on different substrates is not known. The extrapolated values of the diffusion constants at room temperature ($4.1412\times10^{-30}m^2/s$ and $1.3417\times10^{-22}m^2/s$, respectively, for layers on pure Zr and Zr-2.5 Nb [30]) differ greatly, because of the factor of 2 difference in the activation energy (100.1 kJ/mol and 53.7 kJ/mol, respectively).

The calculated diffusion constant of hydrogen in zirconia is of the same magnitude as the measured hydrogen diffusion constants (extrapolated to 1700 K) in oxides grown on Zircaloy-2 ($81.7\times10^{-10}m^2/s$) and Zr-15 Nb ($35\times10^{-10}m^2/s$) [31].

There have been other recent studies of hydrogen diffusion in various oxidized zirconium alloys [32]. The diffusivity at room temperature varied between $1.26\times10^{-12}m^2/s$ and $1.51\times10^{-12}m^2/s$, and decreased as the relative fraction of tetragonal zirconia increased (between 0.9% and 12%). It was also suggested that charged (positive) precipitates created during zirconium oxidation may act as hydrogen traps and lower diffusivity. The higher diffusion of hydrogen in zirconia alloys was attributed to the diffusion through the interconnected pores and unoxidized regions [30]. Our calculations probably overestimate hydrogen diffusion in zirconia because the potential used currently predicts a lower binding energy between hydrogen and oxygen, but studies of hydrogen dissolution [33] and release in nonmetals (uranium dioxide) show a solubility dependence on the square root of the gas pressure, which indicates hydrogen dissolution in atomic form. Also, the principal form of hydrogen released was H_2 with very little water observed [33]. Extrapolated to 1700 K, the measured value of hydrogen diffusion in urania is $5.3\times10^{-8}m^2/s$ [34], which is two orders of magnitude higher than calculated here for hydrogen diffusion in zirconia.

ELECTRON DENSITY AND HYDROGEN DIFFUSION

It is interesting that hydrogen, which diffuses readily into metals, stays on ZrO_2 surfaces and its diffusion in zirconia is smaller, by orders of magnitude, than that in pure zirconium. The trapping of hydrogen in the presence of oxygen can be understood in terms of the change in electron density as the zirconium is oxidized. The electronic-structure calculations for pure zirconium and ZrO_2 were performed (at a temperature of 0 K) using a tight-binding linear muffin-tin orbital atomic-sphere approximation [35] and the calculated total densities of states are shown in Figures 3a and 4a, respectively. The corresponding electron charge densities of zirconium and ZrO_2 are shown in Figures 3b and 4b. It can be seen that the electron densities in metallic zirconium are evenly distributed between 0.02 and 0.05 Bohr-3, whereas in zirconia, electrons are shifted towards oxygen with minimum and maximum densities of 0.01 and 0.16 Bohr-3, respectively. Interestingly, as shown by Nørskov [36], the hydrogen energy is strongly dependent on the electron density within which it is embedded. Thus, it can be shown that hydrogen can become trapped in zirconia at the electron densities where its energy is at a minimum (i.e., when surrounded by a high energy barrier as created by high electron densities from oxygen). Hence, these electron-density calculations support the claim that hydrogen can be trapped on the surface of zirconia as observed in the current simulations.

SUMMARY

Semi-empirical atomistic simulations and *ab initio* electronic structure calculations indicate that oxygen and hydrogen cannot diffuse effectively through a slab of pure ZrO_2. To account for the observed diffusivity of oxygen in zirconium dioxide, diffusion must be taking place through cracks or other defects (e.g. cracks, porosities) where gas diffusion may play the role. It is also found that zirconium vacancies are needed for oxygen diffusion to occur in zirconia. By doping zirconia with Y or Ca, a charge imbalance is created, and to fulfill the charge neutrality oxygen vacancies are created, which will enhance oxygen diffusion. To study the effect of impurities on the diffusion of oxygen and hydrogen in doped zirconia, *ab initio* simulations must be considered due to the complexity of interactions between the atoms.

ACKNOWLEDGEMENTS

Part of the present analysis, which was published previously [3], was supported by the Natural Sciences and Engineering Research Council of Canada and the Department of National Defense (Director General of Nuclear Safety and Academic Research Program). One of the authors (Dr. B. Szpunar) acknowledges support by Dr. B.J. Lewis (in the beginning of this work) and RMC (especially T. Winsor & M. Watt) for providing free access to computer facilities. The authors would like to thank Drs. B.J. Lewis, R.S. Dickson, L.W. Dickson, D.B. Sanderson, F.C. Iglesias, D. Khatamian, W.H. Hocking, D. Than, V. Krstic and J. Szpunar for many helpful comments and discussions, and Dr. O. Jepsen and MPI - Stuttgart for providing the TB-LMTO-ASA code. M.I. Baskes acknowledges support from the USDOE.

REFERENCES

1. Szpunar, B., Lewis, B.J., Arimescu, V.I., Dickson, R.S., and Dickson, L.W., "Three-Component Gas Mixture Transport in Defective CANDU Fuel Rods", J. Nucl. Mater., **294,** 315 (2001).
2. Fontana, M.G., "Corrosion Engineering", (Third Edition, McGraw-Hill Book Company, New York), p. 510 (1986).
3. Szpunar, B., Lewis, B.J., Arimescu, V.I., Dickson, R.S., Dickson, L.W. and Baskes, M.I., "Three-Component Gas Mixture Transport in Defective Candu Fuel Rods", 7th International Conference on CANDU Fuel, Kingston, Ontario, Canada, Conference Proceedings vol. 1, 329, September 23-27, (2001).
4. Jochym, P.T. and Parlinski, K., "Elastic Properties and Phase Stability of AgBr Under Pressure", Phys. Rev. B **65**, 24106 (2002).

5. Baskes, M.I., “Modified Embedded-Atom Potentials for Cubic Materials and Impurities”, Phys. Rev. **B 46,** 2727 (1992).
6. Colomban, P., “Proton Conductors”, (Cambridge University Press) (1992).
7. Baskes, M.I. and Johnson, R.A., “Modified Embedded Atom Potentials for HCP Metals”, Modelling Simul. Mater. Sci. Eng., **2**, 147 (1994).
8. Rose, J.H., Smith, J.R., Guinea, F. and Ferrante, J., “Universal Features of the Equation of State of Metals”, Phys. Rev. **B 29**, 2963 (1984).
9. Huang, H., Ghoniem, N.M., Wong, J.K. and Baskes, M.I., “Molecular Dynamics Determination of Defect Energetics in β-SIC Using Three Representative Empirical Potentials”, Modelling Simul. Mater. Sci. Eng. **3**, 615 (1995).
10. Wyckoff, R.W.G., “Crystal Structures”, (John Wiley & Sons) (1963).
11. Mueller, W.M., Blackledge, J.P. and Libowitz, G.G., “Metal Hydrides”, (Academic Press) (1968).
12. Shackelford, J.F., Alexander, W. and Park, J.S., “Materials Science and Engineering Handbook”, (CRC Press, Boca Raton, Ann Arbor, London, Tokyo) (1992).
13. Buschow, K.H.J., Bouten, P.C.P. and Miedema, A.R., “Hydrides Formed From Intermetallic Compounds of Two Transition Metals: a Special Class of Ternary Alloys”, Rep. Prog. Phys. **45,** 937 (1982).
14. Brandes, E.A., “Smithells Metals Reference Book”, (Butlerworths, London) (1983).
15. David, W.O., Gillis, H.P. and Nachtrieb, N.H., “Principles of Modern Chemistry”, (Harcourt College Publisher) (1999).
16. Szpunar, B., Strange, P. and Wallace, W.E., “Binding Energy and Magnetism of Transition Metal Hydrides”, J. Less-Common Met. **128,** 143 (1987).
17. Dwivedi, A. and Cormack, A.N., “A Computer Simulation Study of the Defect Structure of Calcia-Stabilized Zirconia”, Phil. Mag. **61,** 1 (1990).
18. Kandil, H.M., Greiner, J.D. and Smith, J.F., “Single-Crystal Elastic Constants of Yttria-Stabilized Zirconium in the Range 20 to 700°C”, J. Am. Soc. **67,** 341 (1984).
19. Smith, C.F. and Crandall, W.B., “Calculated High-Temperature Elastic Constants for Zero Porosity Monoclinic Zirconia”, J. Am. Cer. Soc. **47,** 624 (1964).
20. Mackrodt ,W. C. and Woodrow, P. M., “Theoretical Estimates of Point Defect Energies in Cubic Zirconia”, J. Am. Ceram. Soc. **69,** 277 (1986).
21. Nevitt, M. V., Chan, J.Z., Liu, J.Z., Grimisditch, M.H. and Fang, Y., “The Elastic Properties of Monoclinic ZrO_2”, Physica **B150,** 230 (1988).
22. Parker, D.S. and Huffine, C.I., “Properties of Hydrided Zirconium”, USAEC, Report APEX-561, General Electric Company (1959).
23. Cohen, R.E., Mehl, M. J. and Boyer, L.L., “Phase Transitions and Elasticity in Zirconia”, Physica **B150,** 1 (1988).
24. Iglesias, F.C., Sagat, S. and Sills, H.E., “High Temperature Oxidation of Zircaloy”, Res. Mechanica **17,** 125 (1986).
25. Brossman, U., Wurschum, R., Sodervall, U. and Schaefer, H-E., “Oxygen Diffusion in Ultrafine Grained Monoclinic ZrO_2”, J. Appl. Phys. **85,** 7646 (1999).
26. Alta, C.R. and Kwok Chee-Kin, “Fundamental Optical Absorption Edge of Sputter-Deposited Zirconia and Yttria”, J. Am Ceram. Soc. **73,** 3209 (1990).
27. Stotz, S. and Wagner, C., “Solubility of Water Vapor and Hydrogen in Solid Oxides”, Ber. Bunsenges. Physik. Chem. **70,** 781 (1966).

28. Hashizume, K., Sugisaki, M., Hatano, K., Ohmori, T. and Ogi, K., "Application of Discharge Implantation Method to Measurement of Diffusion Coefficient of Hydrogen Isotopes in Zirconium", J. Nuclear Science and Technology, **31,** 1294 (1994).
29. Kearns, J.J., "Diffusion Coefficient of Hydrogen in Alpha Zirconium, Zircaloy-2 and Zircaloy-4", J. Nucl. Mater. **43,** 330 (1972).
30. Khatamian, D. and Manchester, F.D., "An Ion Beam Study of Hydrogen Diffusion in Oxides of Zr and Zr-Nb (2.5 wt%)", J. Nucl. Mater. **166,** 300 (1989).
31. Khatamian, D., "Hydrogen Diffusion in Oxides Formed on Surfaces of Zirconium Alloys", J. Alloys and Comp. **253-254** 471 (1997).
32. Hyuck, L.B., Seon, H.H. and Sub, L.K., "Measurements of Hydrogen Permeation and Absorption in Zirconium Oxide Scales", J. Nucl. Mater. **312** 134 (2003).
33. Sherman, D.F. and Olander, D.R., "Hydrogen Dissolution in and Release from Nonmetals, I. Uranium Dioxide", J. Nucl. Mater. **166,** 307 (1989).
34. Wheeler, V.J., "The Diffusion and Solubility of Hydrogen in Uranium Dioxide Single Crystals", J. Nucl. Mater. **40,** 189 (1971).
35. Andersen, O.K., Jepsen, O. and Sob, M., in *Electronic Band Structure and its Applications* (edited by M. Yussouff, Springer Verlag, Berlin),1 (1986).
36. Nørskov, J.K., "Chemisorption on Metal Surfaces", Rep. Prog. Phys. **53,** 1253 (1990).

Table 1: Parameters for the Elements Zr, O and H[a]

Element	E_c	r_e	α	A	$\beta^{(0)}$	$\beta^{(1)}$	$\beta^{(2)}$	$\beta^{(3)}$	$t^{(0)}$	$t^{(1)}$	$t^{(2)}$	$t^{(3)}$	ρ_0
Zr	6.325	3.21	4.46	1.03	3.7	1.0	5.7	1	1	5	4.5	-3.5	0.63
O	2.558	1.21	6.49	1.5	6.49	6.5	6.5	6.5	1	0.09	0.1	0	6.5
H	2.235	0.74	2.96	2.5	2.96	3.0	3.0	3.0	1	0.2	-0.1	0	16

a. Values listed are the cohesive energy E_c (eV), the equilibrium nearest-neighbor distance r_e (Å), the exponential decay factor α for the universal energy function, the scaling factor A for the embedding energy, the exponential decay factors β for the atomic densities, the weighting factors t for the partial electron densities, and the atomic density scaling factor ρ_0.

Table 2: Parameters for the Binary UBER[a]

Compound	E_c (eV)	r_e (Å)	α
ZrO	5.76	2.185	4.22
ZrH	3.23	2.06	3.92
OH	2.15	0.971	4.6

a. The parameters are defined in Table 1.

Table 3: Lattice Constants (a, c), Cohesive Energy (E_c) Per Atom and Energy of Zirconium Oxygen, Hydrogen or ZrA-Type Vacancies[a]

Parameters	ZrO_2		ZrH_2	
	Calculated	Experimental	Calculated	Experimental
a (Å)	5.07	5.07 [10]	4.83	4.981 [11]
c(Å)				4.451 [11]
E_c (eV)	7.63	7.63 [12,14,15] 5.51 [12,15]	4.18	4.19 [13,14,15] 2.07 [13,15]
V_{Zr} (eV)	24.36		10.57	
V_A (eV)	11.33		6.04	
V_{ZrA} (eV)[b]	32.49		15.15	

a. The calculated values are at 0 K temperature.

b. V_{ZrA} corresponds to the nearest neighbor atom. An A-type atom corresponds to either an oxygen or hydrogen atom in ZrO2 and ZrH2.

Table 4: Elastic Properties

Property (in GPa)[a]	ZrO_2			ZrH_2		
	Calculated		Experimental	Calculated		Experimental
	VASP	MEAM		VASP	MEAM	
B	235 (230)	218	194 [18][c]	133 (130)	134	60
G	99	86	95 [18][c] 96-113 [19][a]	33	36	
Y	261	228	204.93 [12][c] 244-257 [19][a]	93	74	82.8 [22][d]
c_{11}	489	482	417 [18][c] 400.9 [20][b] 341 [21][a]	164	210	
c_{12}	108	86	82 [18][c] 113 [21][a]	118	96	
c_{44}	62	45	47[18][c] 103 [21][a]	43	26	

a.. The measurements are for the monoclinic phase.

b. Stabilized zirconia

c. Extrapolated to pure zirconia from stabilized zirconia results.

d. The measurements are for 50.6% hydrogen in zirconium hydride.

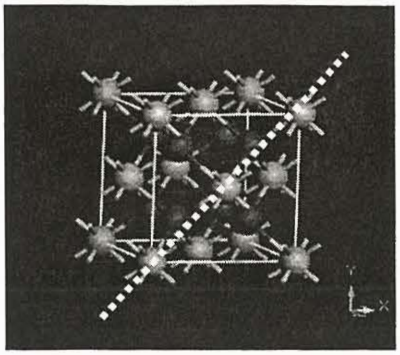

Figure 1
Unit cell of ZrO_2 (light and dark shade of gray balls are zirconium and oxygen atoms, respectively). The dotted line indicates cross section used for (110) surface diffusion studies.

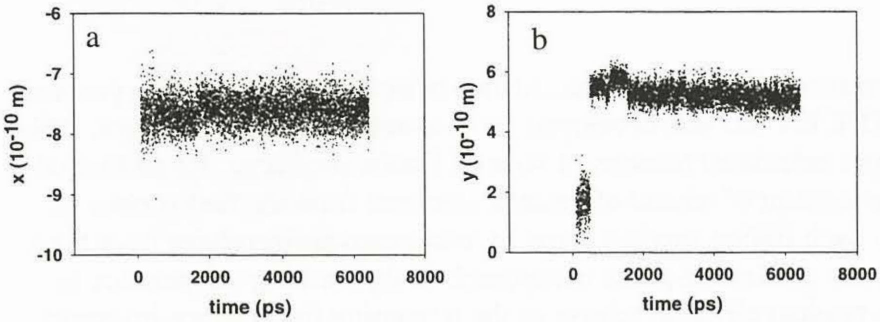

Figure 2a-b
The x (a) (direction [001]) and y (b) ([010]) coordinates (as a function of time) of one of the atoms on (110) surface.

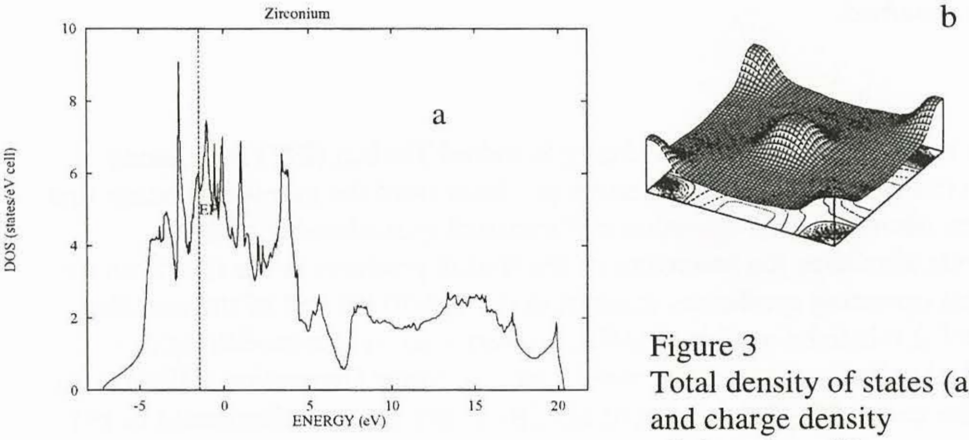

Figure 3
Total density of states (a) and charge density of zirconium (b).

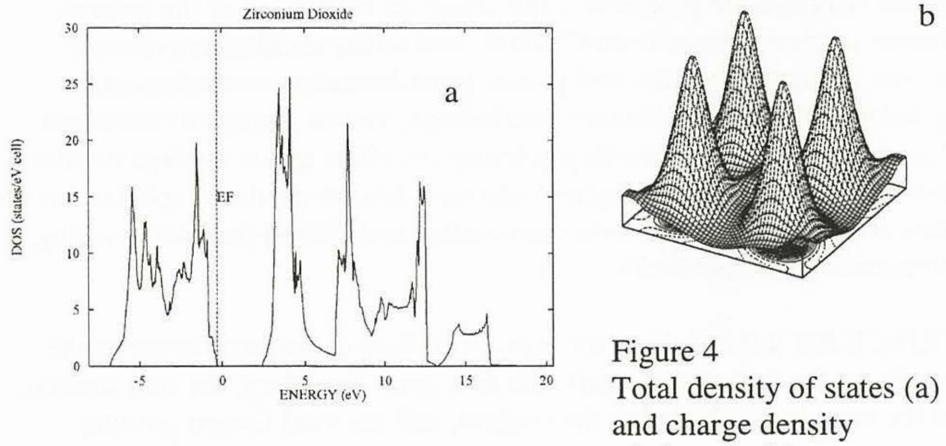

Figure 4
Total density of states (a) and charge density of zirconia (b).